Langmuir

Article

pubs.acs.org/Langmuir

Fabrication and Characterization of Dendrimer-Functionalized Mesoporous Hydroxyapatite

Nabakumar Pramanik[†] and Toyoko Imae*[,†,‡]

[†]Graduate Institute of Applied Science and Technology and [‡]Department of Chemical Engineering, National Taiwan University of Science and Technology, Taipei 10607, Taiwan

ABSTRACT: A successful synthesis of mesostructured hydroxyapatite (HAp) using cetyltrimethylammonium bromide and poly(amido amine) dendrimer porogens has been reported. A comparative study of physicochemical properties has also been performed. The formation of a single-phase hydroxyapatite crystal in synthesized HAp particles with an aspect ratio of 2.3 was revealed. The formation of the mesostructural nature of HAp was proven with a specific surface area (56−63 m^2/g) and a certain pore size (4.7−5.5 nm), although there were significant differences between particles from surfactant micelle and dendrimer porogens. In addition, the surface modification of mesoporous HAp particles was carried out using poly(amido amine) dendrimer. The content and thickness of the dendrimer coating on particle surfaces were highly dependent on the pH. At pH 9 or greater, the coating thickness corresponded to at least a double layer of dendrimer, but it decreased sharply with decreasing pH from 9 to 6, in agreement with the protonation of amine groups in the dendrimer, indicating the strong interaction of nonionic dendrimer with HAp. The developed dendrimer-functionalized mesoporous hydroxyapatite materials may be applicable in biocomposite material and/or bone tissue engineering.

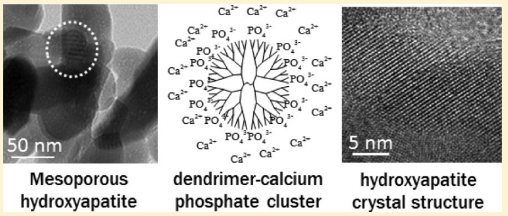

1. INTRODUCTION

During the past decade, mesoporous materials have attract much attention because of their unique surface and textural properties such as high surface areas, small, tunable pore sizes, and large pore volumes, which are crucial for developing new types of catalysts, adsorbents, drug delivery systems, and so on.[1,2] Since the development of silicate-based mesoporous material,[3] its investigation has been one of the most energetic research areas in materials science. In addition, mesoporous materials can be considered to be excellent candidates for osteoanagenesis materials for two major reasons: (i) The porosity and pore volume of biomaterials allow the growth of bone tissues to accomplish full integration with living bones, and they strongly support the formation of bonelike apatite on their surfaces after soaking in simulated body fluids.[4] (ii) The mesoporous structure has the potential to incorporate large numbers of biologically active molecules, including osteogenic agents that can promote drug delivery and bone tissue regeneration.[5]

Hydroxyapatite $[Ca_{10}(PO_4)_6(OH)_2]$ (HAp), which is the major inorganic component of bone and teeth, is a key biomaterial in potential orthopedic, dental, and maxillofacial therapies because of its excellent biocompatibility, bioactivity, and osteoconductivity.[6] Moreover, HAp's are useful as drug carriers for the delivery of a variety of pharmaceutical molecules because of their nontoxic and noninflammatory properties.[7]

The investigation to mimic the natural growth of bone first concentrated attention on the synthesis of HAp-based biomaterials with porous morphology (such as those with pore sizes of 50−500 μm),[8−12] which was performed by plasma spray,[8] by solid-state reaction,[9,10] and through a suspension−precipitation route.[11,12] The increase in surface area resulting from the porosity will contribute to the capacity of delivery agents to adsorb a drug, and these porous structures must be significant in biomedical applications because they can enhance the adhesion of the apatite implant to the bone. In fact, porous HAp's possessed their adsorbing properties toward various substances.[8] Porous HAp's with cylindrical pores could be a useful graft material because of their strength, osteoconductivity, and easily controllable pore geometry.[9] The pores of HAp's could be substituted with functional groups to modify their surfaces, and their porosity could also facilitate the incorporation of substituents.[10] Porous HA was also utilized for the fabrication of ocular implants and for bone tissue engineering.[11,12]

In recent years, particular attention has been paid to the preparation of mesoporous HAp's by using a templating route.[13−18] When silica, yeast cells, and $CaCO_3/Fe_3O_4$ microsphere were utilized as templates, the particle sizes of HAp's were small (2.7−4.5 nm[14−16]), whereas HAp's templeated with polymers (EOmPOnEOm) exhibited large pore sizes (14 to 15 nm).[16−18] These mesoporous HAp's could be used in drug loading/release,[16] protein loading/delivery,[17] and opthopedic applications.[18] In the meantime, the fabrication of mesoporous materials with well-ordered pores was developed using a template of cetyltrimethylammonium bromide (CTAB) micelles,[19] and such a procedure was applied even for the preparation of mesoporous HAp but the produced particle had a rather large pore (~40 nm),[13] different from mesoporous silica (3.2 nm).[19] Because dendrimers take a

Received: May 21, 2012
Revised: September 3, 2012
Published: September 4, 2012

Scheme 1. Scheme of the Formation Process of Mesoporous HAp Powders Using Micelle and Dendrimer Porogens

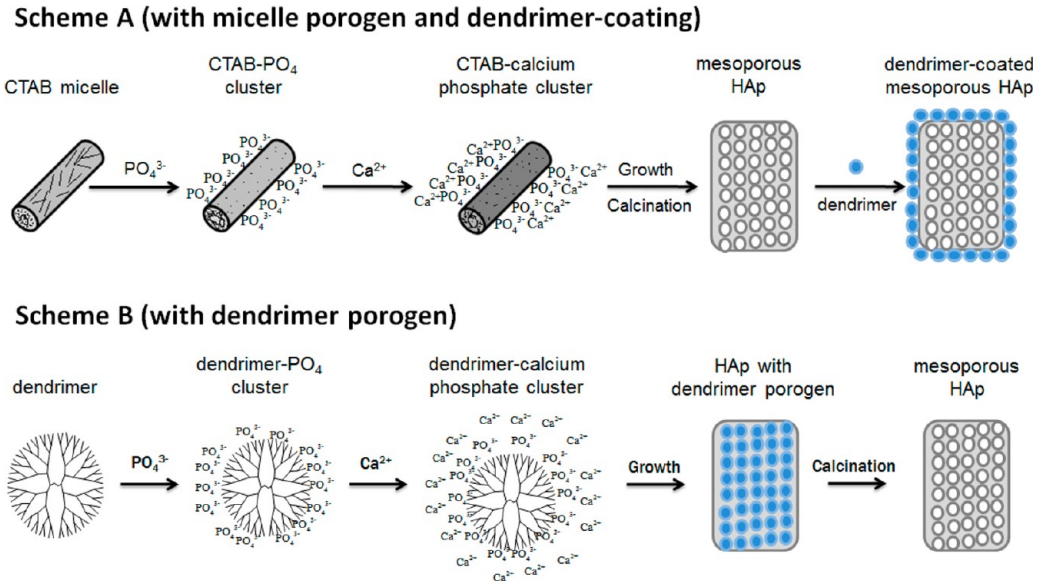

monomolecularly micellelike structure, they should be useful as a simple template, and they were actually used as a template in the preparation of mesoporous materials.[20] However, there is no report relating to mesoporous HAp's templated by dendrimers, so there is the need for further investigations of mesoporous HAp materials. Such studies are useful to improving the quality of materials for bone tissue engineering.

The surface modification of particles is an efficient way to obtain materials having specific properties and to improve the surface activity as well as the functionality.[21] The surface modification of HAp appears to be of great interest owing to the unique activities of this mineral in biomaterials. The unique activities are ascribed to the surface properties of HAp, such as surface functional groups, acidity or basicity, surface charge, solvophilicity, and porosity. Thus, the modification of the HAp surface is expected to control the surface structure and properties, leading to the provision of a novel function to HAp. A variety of investigations have been reported for methodologies such as the adsorption of carboxylic acid,[22] isocyanate,[23] and sulfonate[24] on the particle surfaces. Meanwhile, some researchers have also reported the surface modification of HAp with alkyl phosphate,[25] hexanoic and decanoic acids,[26] and hexamethyldisilazane[27] for the purpose of using this material as a filler in cements, polymers, and bioceramics. Also, a silane coupling agent,[28] a zirconyl salt,[29] a polyacid,[30] and poly(ethylene glycol)[31] have also been applied to modify the surface of HAp.

Thus, it is anticipated that the modification of the HAp surface with various organic and inorganic substances imparts novel functions to HAp and improves the mechanical properties and affinity to the target materials if HAp is used as a filler. Moreover, it should be possible to extend and fine tune the bioactivity of such nanoparticles by surface functionalization using water-soluble macromolecules. However, although numerous HAp composites have been explored,[22−31] a basic study of HAp composites with dendrimers has never been reported. A new architecture of synthetic polymers, namely, dendrimers, is composed of a core, branches extending from the core, and terminal groups, and dendrimers have multiple functionalities, especially at the terminals that are all available for chemical reactions or interactions.[32] This character can be advantageous in tissue engineering: the multiple functionality of the dendrimer will allow an increased number of interactions with the HAp ceramics. These interactions may strengthen the matrix and can aid in limiting the crystallization of HAp. The increased number of interactions also allows for the increased strength of HAp within the composite or matrix.

In this regard, poly(amido amine) (PAMAM) dendrimers with surface amine groups are ideal candidates for the production of bioinorganic HAp nanoparticles and nanocomposites because of their relatively low toxicity, intrinsic biocompatibility, and interaction ability with surfaces.[33] PAMAM dendrimers can be regarded as mimics of ionic micelles and proteins[32] or globular polyelectrolytes and build complexes with nucleic acids.[34,35] Because of the unique and well-defined secondary structure of the dendrimers, they can be good candidates for studying inorganic crystallization.[36] The interaction of the surfaces of dendrimers with metal ions was examined,[37] and PAMAM dendrimers were used as templates and protectors for the formation of metal nanoparticles.[38,39] The effect of the anionic PAMAM dendrimer with carboxylate terminal groups was also found on the crystallization of $CaCO_3$ particles.[40] Thus, all of the studies elucidate that dendrimers can be successfully employed for the production of HAp composite materials.

The present research consists of the development of dendrimer-functionalized mesoporous hydroxyapatite. Mesoporous HAp's using CTAB and PAMAM dendrimer as a template were synthesized through a chemical-based hydrothermal method. The physicochemical properties of the synthesized powders were investigated. Afterwards, the surface of mesoporous HAp was functionalized with PAMAM dendrimer using an aqueous-based chemical method. The synthesized materials were characterized through various measurements. To the best of our knowledge, there is no report on the development of dendrimer-functionalized mesoporous HAp in the literature.

dx.doi.org/10.1021/la302066e | Langmuir 2012, 28, 14018−14027

2. MATERIALS AND METHODS

2.1. Chemicals. All chemicals used were of analytical grade and available from commercial sources. Calcium nitrate (99+%) and diammonium hydrogen phosphate (99+%) were purchased from Acros Organic, USA. CTAB was a product of TCI-EP, Japan. An aqueous NH_3 solution (35 v/v%) was obtained from Fisher Scientific Limited, U.K. Amine-terminated PAMAM dendrimer (generation 4, 10 wt % solution in methanol) was purchased from Sigma-Aldrich, USA. Methanol was evaporated before preparing an aqueous dendrimer solution. Milli-Q (deionized and distilled) water was used throughout the experiments.

2.2. Synthesis of Mesoporous HAp Powders. Mesoporous HAp powders were synthesized through a hydrothermal method. In a typical procedure for the preparation of mesoporous HAp powders, each 0.5 M stock solution of calcium nitrate [$Ca(NO_3)_2{\cdot}4H_2O$] and diammonium hydrogen phosphate [$(NH_4)_2HPO_4$, DAHP] was prepared in water. CTAB powder as a porogen surfactant was mixed with a DAHP solution (1:1 mol/mol PO_4^{3-}/CTAB) and allowed to stir for 1 h. Subsequently, the CTAB–phosphate solution at a Ca^{2+}/PO_4^{3-} composition number ratio of 1.67 was added dropwise to the calcium nitrate solution with vigorous stirring by a magnetic stirrer at room temperature. The pH of the reacting mixture was always maintained at around 11 to 12 with the addition of an NH_3 solution before and after mixing the Ca^{2+} and PO_4^{3-} solutions. A colloidal suspension with white precipitates was obtained, and it was then transferred to a Teflon tube (80 cm^3). The tube was held in a stainless steel autoclave, sealed, and maintained at 150 °C for 15 h for annealing. After the autoclave cooled to room temperature, the precipitate was separated by filtration and washed with water and ethanol in sequence. Finally, the precipitate was dried in an oven at 90 °C overnight. The dried precipitate was then ground with a mortar and a pestle and calcined at 600 °C for 6 h to remove a porogen. Similarly, HAp powders were also synthesized using the PAMAM dendrimer (1:1 mol/mol PO_4^{3-}/terminal amine of dendrimer) as a porogen via the same method as for the CTAB porogen and calcined at 600 °C for 8 h to remove the PAMAM dendrimer. Separately, HAp powder was synthesized without porogen. The preparation procedures of HAp's are represented in Scheme 1.

2.3. Surface Functionalization of HAp Powders with PAMAM Dendrimer. PAMAM dendrimer (0.1 g) was solvated in 10 cm^3 of water, and the pH of the solution was adjusted to 10 to 11 by adding an aqueous NH_3 solution. The solution was stirred with a magnetic stirrer for 30 min. Then, calcined HAp powders (prepared by using a micelle porogen) (0.6 g) were gradually added to the dendrimer solution (20 cm^3) with vigorous stirring using a magnetic stirrer at room temperature. After the addition of entire nanoparticles, the mixture was allowed to stir overnight, followed by sonication for 30 min using a high-power ultrasonic device (Branson, Yamato-1210, Japan). The product was separated by filtration (Whatman-41), followed by washing with an ethanol–water mixture, and then dried overnight in a vacuum oven at 50 °C. Dendrimer-modified HAp powders were prepared at different pH values. Scheme 1 includes the procedure.

2.4. Characterization. The identification of functional groups in HAp, HAp with CTAB porogen (HAp/CTAB), and HAp with dendrimer porogen (HAp/PAMAM) powders was analyzed by Fourier transform infrared (FTIR) absorption spectroscopy (Nicolet 6700, USA) within the scanning range of 4000 to 400 cm^{-1} using a KBr pellet technique. The phase analysis of powders was done with an X-ray diffraction (XRD) instrument (PSAXS-USH-WAXS-002, Osmic, USA) using a 0.67 mA current and 45 kV voltage with monochromatic Cu Kα (target) radiation (λ = 1.5405 Å) with a step size of 0.05° 2θ, a scan rate of 0.03° 2θ/s, and a scan range from 2θ = 20 to 60°. The XRD technique was also employed to determine the average domain size of HAp crystals. Small-angle XRD patterns were also recorded on the same instrumental system and under conditions over the range of 0.5° ≤ 2θ ≤ 10°. The molar ratio of calcium/phosphorus (Ca^{2+}/PO_4^{3-}) HAp powder was measured with an energy-dispersive X-ray (EDX) analyzer (JEOL, JSM-6500F, Japan). The textural properties of synthesized powders were analyzed by the nitrogen adsorption experiment at 77 K using a surface area analyzer (Micromeritics Tristar 3000 porosimeter, Australia) after the samples were degassed at 125 °C for 3 h. The morphology and the particle size of the powders and the coating thickness of the PAMAM dendrimer on the power surfaces were observed with a Hitachi (H-7000, Japan) transmission electron microscope (TEM) at an acceleration voltage of 100 kV. The TEM specimens were prepared by depositing a drop of an HAp powder dispersion, which was prepared in ethanol by ultrasonication for 20 min, on a carbon-coated copper grid and by drying at room temperature. The thermogravimetric (TG) analysis was carried out on a TG/DTA thermal analyzer (TGA Q500, U.K.). Using 100 mL/min air/N_2 flow, the temperature was raised to 800 °C at a constant rate of 10 °C/min.

3. RESULTS AND DISCUSSION

Mesoporous HAp powders were synthesized through a hydrothermal method using a CTAB micelle or PAMAM dendrimer porogen following the procedures in Scheme 1. FTIR spectra of HAp with CTAB micelle porogen before and after calcination are shown in Figure 1A. IR bands at 3572 and 632 cm^{-1} belong to the vibrational mode of structural OH

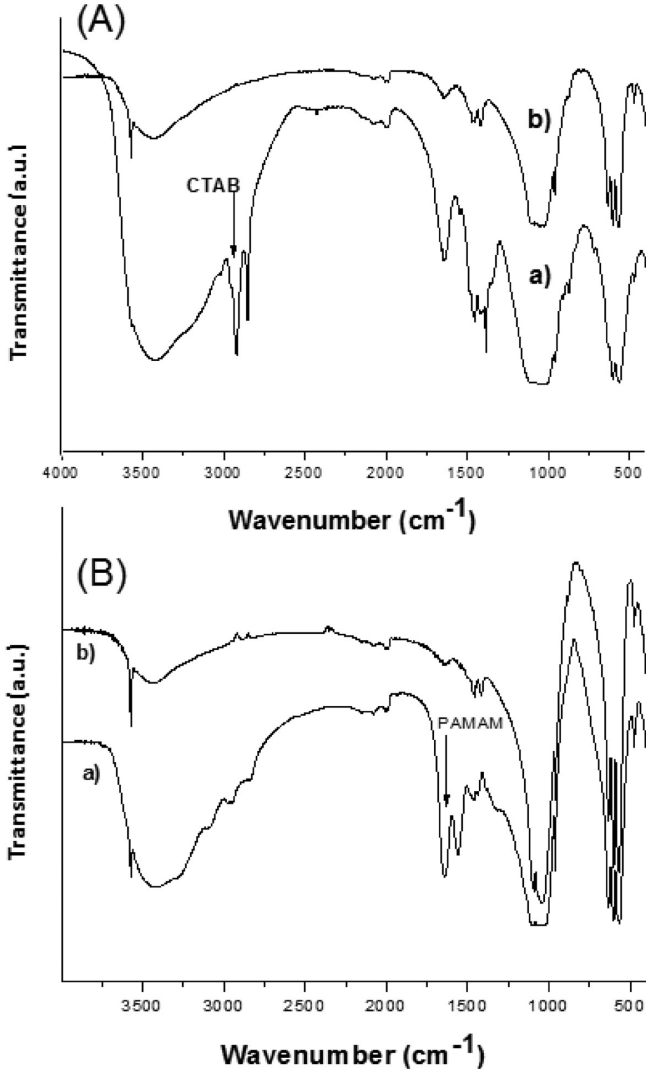

Figure 1. FTIR spectra of HAp powders. (A) From the CTAB micelle porogen and (B) from the PAMAM dendrimer porogen. (a) Before calcination and (b) after calcination.

dx.doi.org/10.1021/la302066e | Langmuir 2012, 28, 14018–14027

groups of hydroxyapatite (Figure 1Aa). The bands at 1093, 1036, and 962 cm^{-1} are characteristic of the phosphate stretching vibrational modes (γ_3, γ_3, and γ_1 of PO_4^{3-}, respectively), and the bands observed at 602, 565, and 472 cm^{-1} are due to the phosphate bending vibrational modes (γ_4, γ_4, and γ_2 of PO_4^{3-}, respectively).[41] Bands assigned to the carbonate anion are also observed at 1456 and 1408 cm^{-1}, resulting from the dissolved CO_2 from the atmosphere during mixing, stirring, and precipitating materials.[42] The strong absorption bands at 2954 and 2848 cm^{-1} are assigned to CH_2 stretching modes of CTAB.[43] After the calcination at 600 °C, the strong bands at 2954 and 2848 cm^{-1} have vanished (Figure 1Ab), implying no residual CTAB species in the calcined sample. However, amide I and II bands at 1651 and 1553 cm^{-1}, respectively, in Figure 1Ba represent the presence of the PAMAM dendrimer in the HAp particles prepared using the PAMAM dendrimer as a porogen.[44] However, these bands were imperceptible after the powders were calcined at 600 °C (Figure 1Bb). This phenomenon indicates that by using the calcination method, the CTAB micelle or PAMAM dendrimer template in HAp solids can be removed completely.

X-ray diffraction patterns of calcined HAp powders are presented in Figure 2. The main crystalline peaks observed for

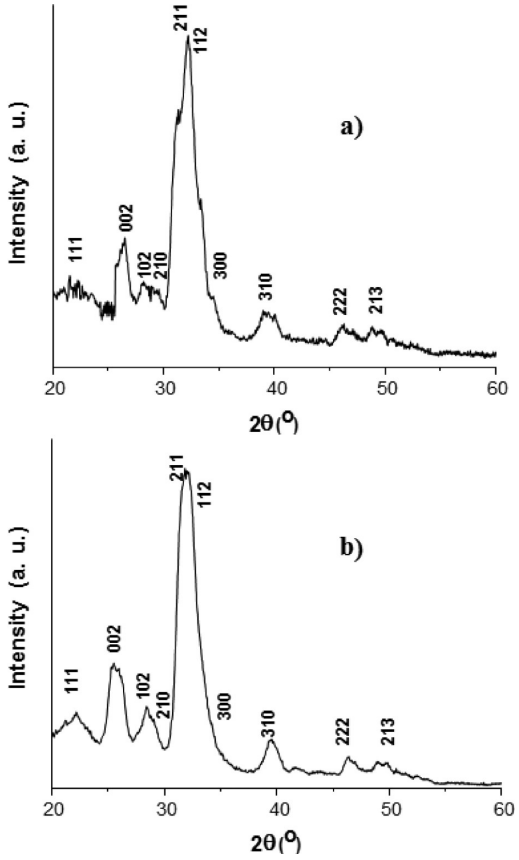

Figure 2. XRD of calcined HAp powders. (a) From the micelle porogen and (b) from the dendrimer porogen.

HAp are at diffraction angles of 26.26, 31.96, 32.35, 34.48, 39.85, and 46.61° with d spacing of 3.44, 2.80, 2.73, 2.63, 2.26, and 1.94 Å, respectively, for calcined HAp powder from the CTAB micelle porogen (Figure 2a). In the case of calcined HAp powder from the PAMAM dendrimer porogen, the crystalline peaks were observed at slightly different diffraction angles of 25.49, 31.79, 31.86, 34.09, 39.66, and 46.39° with d spacings of 3.53, 2.81, 2.74, 2.69, 2.29, and 1.96 Å, respectively (Figure 2b). These d values correspond to that of hexagonal HAp with a space group of $P6_3/m$ [$Ca_{10}(PO_4)_6(OH)_2$] (JCPDS-International Center for Diffraction Data, card no. 09-0432) for both calcined HAp powders from micelles and dendrimers. The broadening of XRD peaks indicates the nanocrystalline nature of the synthesized HAp powders. It is evident from the observed results that no characteristic diffraction angles from other calcium phosphate phases are detected.

The relationship among lattice constants (a and c), Miller's indices (h, k, l), and lattice spacing (d) is used to calculate lattice parameter values:

$$\frac{1}{d^2} = \frac{4}{3}\left(\frac{h^2 + hk + k^2}{a^2}\right) + \frac{l^2}{c^2}$$

The lattice parameters were found to be $a = b = 9.42$ Å and $c = 6.88$ Å for calcined HAp powder from micelle porogens and $a = b = 9.41$ Å and $c = 6.87$ Å for calcined HAp powder from the dendrimer porogen. The results are consistent with the previously reported data.[45] The results obtained from the XRD study are summarized in Table 1. Then, the wide-angle XRD results reveal that the present calcined materials take a hydroxyapatite phase,[46] which is also confirmed by the result raised from FTIR data described above. The result is also supported by energy-dispersive X-ray analysis (EDX): The observed Ca^{2+}/PO_4^{3-} number ratio (1.669 and 1.662) against a calculated value (1.67) indicates that the materials are stoichiometric for both HAp's synthesized using micelles and dendrimers, respectively, as a porogen (Table 2). The average domain size of calcined HAp powder obtained from XRD data was ~56 nm for a powder from the micelle porogen with aspect ratios 2.29 and ~52 nm for the powder from the dendrimer porogen with an aspect ratio of 2.25. The results are summarized in Table 1.

Figure 3 shows low-angle XRD patterns of calcined HAp powders. In Figure 3a for an HAp powder from a micelle porogen, a sharp diffraction peak [100] appeared at a 2θ value of around 1.69°, which corresponds to the d-spacing value of 5.19 nm. Another weak peak [200] became visible at a 2θ value of 2.69°, corresponding to the d-spacing value of 3.29 nm. When the PAMAM dendrimer was used as a porogen, a sharp peak [100] had a 2θ value of around 1.68° having a d spacing of 5.36 nm (Figure 3b). An additional peak [200] observed at a 2θ value of 2.67° corresponds to a d-spacing value of 3.83 nm. The phase plane may result from the ordering of pores generated in the powders.[47] The d spaces obtained indicate that the pores generated in HAp particles using micelle or dendrimer porogens have approximate center-to-center distances (a_o) of 5.99 and 6.19 nm, respectively, if the pore arrangement is hexagonal.[20] The results are summarized in Table 3.

The textural properties of the calcined materials were investigated through BET (Brunauer–Emmett–Teller) surface area analysis and are shown in Figure 4. Figure 4a is the nitrogen adsorption and desorption isotherms of calcined HAp powder from the micelle porogen. The isotherms exhibit a type IV isotherm cycle for mesoporous materials under the BDDT (Brunauer–Deming–Deming–Teller) system with a typical H1 hysteresis loop according to an IUPAC classification[48] and a well-defined step at approximately $P/P_0 = 0.84–0.98$. However, Figure 4b shows the BET isotherms of calcined HAp powder

dx.doi.org/10.1021/la302066e | Langmuir 2012, 28, 14018–14027

Table 1. Numerical Values Obtained from XRD and TEM Studies of Calcined HAp Powders

	XRD lattice parameter (Å)		XRD domain size (nm)		XRD aspect ratio	TEM particle size (nm)		
powder	*a*, *b*	*c*	d_{002}	d_{300}	d_{002}/d_{300}	length	diameter	TEM aspect ratio
HAp from micelle	9.42	6.88	78	34	2.29	89 ± 5	38 ± 6	2.34
HAp from dendrimer	9.41	6.87	72	32	2.25	82 ± 3	36 ± 4	2.28

Table 2. EDX Data of Calcined HAp Powders

element	HAp from dendrimer (atom %)	HAp from micelle (atom %)
P K	37.57	37.46
Ca K	62.43	62.54
Total	100.00	100.00
observed Ca^{+}/PO_4^{3-} number ratio	1.662	1.669
calculated Ca^{+}/PO_4^{3-} number ratio	1.67	1.67

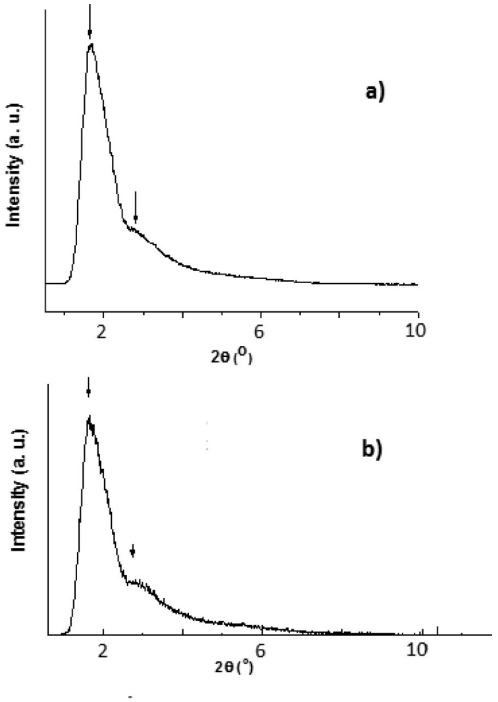

Figure 3. Low-angle XRD of calcined HAp powders. (a) From the micelle porogen and (b) from the dendrimer porogen.

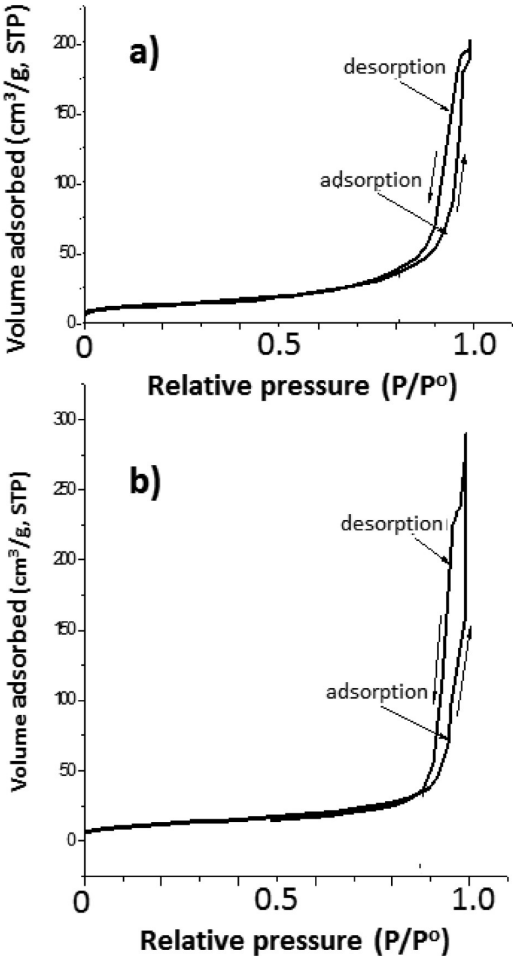

Figure 4. BET N_2 adsorption/desorption isotherms of calcined HAp powders. (a) From the micelle porogen and (b) from the dendrimer porogen.

from the dendrimer porogen. The isotherms were also assigned to the same type as HAp from the micelle porogen and displayed a well-defined step at approximately P/P_0 = 0.86–0.98. The results imply that the synthesized HAp powders are of a mesostructural nature.

The pore size distributions calculated from the desorption branch of the isotherms based on a BJH (Barret–Joyner–Halenda) model are shown in Figure 5a,b for calcined HAp powders from micelle and dendrimer porogens, respectively. The curve indicates a broad pore distribution width with an average size centered on 4.7 ± 0.9 nm for HAp from the micelle porogen. In the case of HAp from the dendrimer porogen, the average size is around 5.5 ± 1.25 nm (Table 3). This type of broad distribution might be raised not only by the mesostructural nature of materials but also by the mode of crystallite aggregates.[49,50] This suggests that the pores are generated through the imprinting of the individual porogen used to obtain HAp powders. Besides, on the basis of the overall investigation of the N_2 adsorption–desorption iso-

Table 3. Numerical Values Obtained from XRD, BET, and TEM Studies for Calcined HAp Powders

	XRD space (nm)			BET isotherm		pore size (nm)	
powder	d_{100}	d_{200}	center-to-center distance (a_o)	specific surface area (m^2/g)	pore volume (cm^3/g)	BET	TEM
HAp from micelle	5.19	3.29	5.99	62.58	0.19	4.7 ± 0.9	4.4
HAp from dendrimer	5.36	3.83	6.19	56.46	0.18	5.5 ± 1.25	5.2

dx.doi.org/10.1021/la302066e | *Langmuir* 2012, 28, 14018–14027

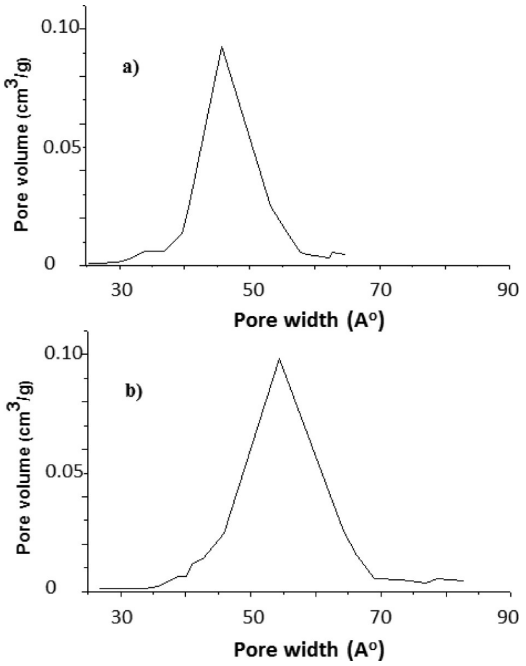

Figure 5. BJH pore size distributions for calcined HAp powders. (a) From the micelle porogen and (b) from the dendrimer porogen.

therms, the specific surface area and pore volume of mesoporous HAp from the micelle porogen were found to be 62.58 m^2/g and 0.19 cm^3/g, respectively. When the dendrimer porogen was used, they were 56.46 m^2/g and 0.18 cm^3/g, respectively.

The morphologies, particle sizes, and pores were investigated through TEM analysis. Figure 6a shows a TEM image of a calcined HAp powder prepared from the micelle porogen. The micrograph depicts short columnar crystals of HAp particles with approximate sizes of 89 ± 5 nm length and 38 ± 6 nm diameter, having an aspect ratio of 2.34. The columnar crystals of HAp particles from the dendrimer porogen are shown in Figure 6b with estimated sizes of 82 ± 3 nm in length and 36 ± 4 nm in diameter with an aspect ratio of 2.28. The aspect ratios obtained from TEM are very similar and are consistent with the values that were obtained from XRD analysis, as seen in Table 1.

The existence of pores and their disordered arrangement are visually observed in the TEM image of calcined HAp from the micelle porogen (Figure 6a). The chaotic arrangement of generated pores in calcined HAp powders from the dendrimer porogen is also exhibited in the TEM image (Figure 6b), but there are also domains where pores are arranged in order (inset circle in Figure 6b). Then the rough evaluation of 5.6−6.0 nm for the center-to-center distance (a_o) is not very far away from the value from XRD (Table 3). Although it was not possible to calculate the exact pore size from the TEM images because of the low resolution of TEM technique, the approximate diameter of the pores was found to be 4.4−5.2 nm for both powders. This result is also consistent with the values obtained from the BET study (Table 3). The diameters of the CTAB micelle and dendrimer are observed to be ∼5.2 and ∼4.5 nm, respectively,[32,51] and the calculated sizes of cetyltrimethylammonium micelle except for the Br ion and dendrimer are 4.2 and 4.0 nm, respectively. Then the pore sizes in HAp are in correlation with the size of the templates. Incidentally, the pore sizes using the dendrimer porogen were 3.2 and 3.9 nm for

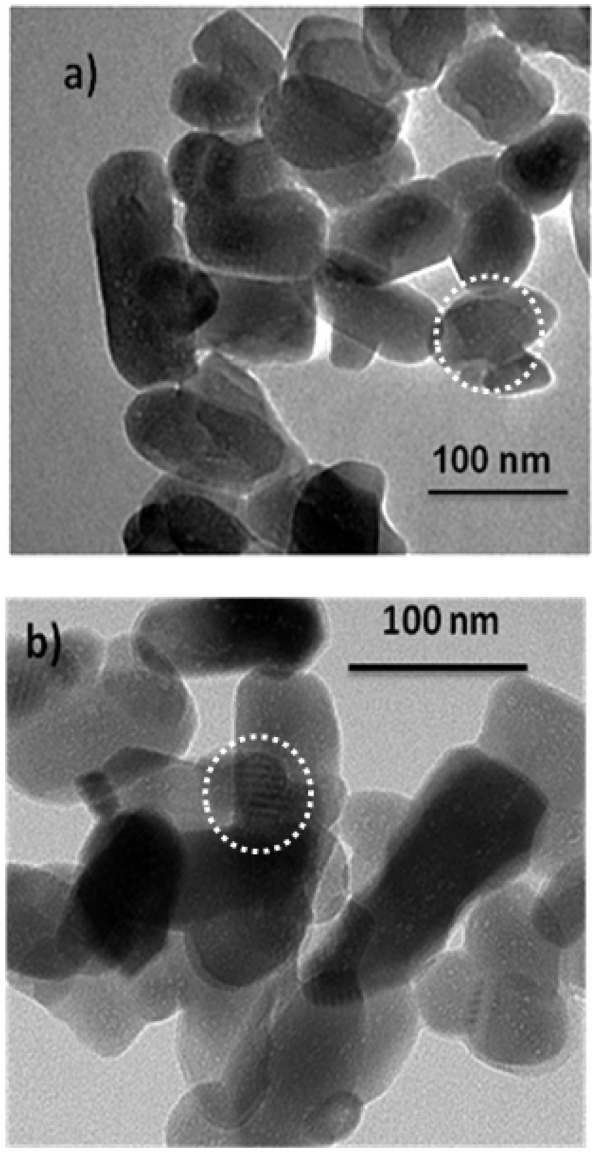

Figure 6. TEM micrographs of calcined HAp powders. (a) From the micelle porogen and (b) from the dendrimer porogen.

$FePO_4$ and tetraethyl orthosilicate particles, respectively,[44,52] and 3.7−4.9 and 5.9−6.8 nm for silatrane particles.[20] High-resolution TEM micrographs for the calcined HAp powders are given in Figure 7. Figure 7a,b displays photographs of HAp powders from micelle and dendrimer porogens, respectively. Both photographs are illustrative of the crystal structures of HAp, approving the results of XRD.

A credible mechanism for the formation of mesoporous structure is presented in Scheme 1. At first, CTAB molecules form micelles in the solution. After the addition of an aqueous PO_4^{3-} solution to the aqueous CTAB solution, the CTAB-PO_4 complex, which consists of many PO_4^{3-} species bound to the surface of the micelle, is formed. After an aqueous Ca^{2+} solution was added, a CTAB−calcium phosphate cluster is formed because of the conformational compatibility between the identical hexagonal shape of the micelle and calcium phosphate.[53] The micelle acts as a nucleating point for the growth of HAp crystals at an adequate aging temperature and time, and the crystals coalesce to form a stable 3D structure of HAp. Then, the mesoporous HAp powders are obtained by

dx.doi.org/10.1021/la302066e | Langmuir 2012, 28, 14018−14027

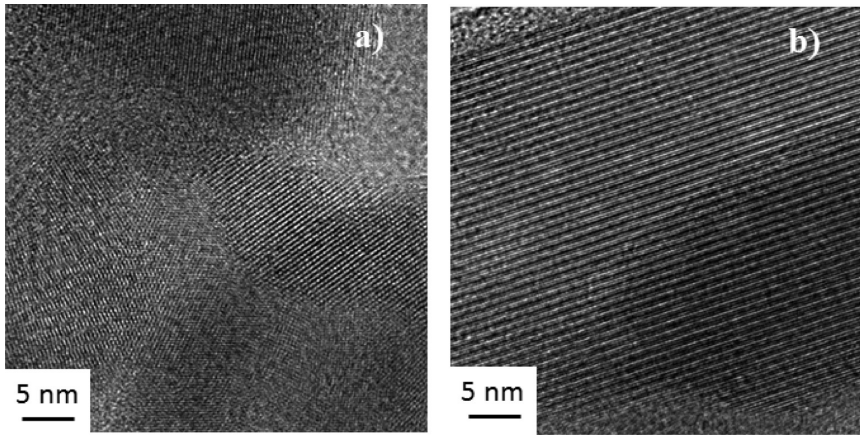

Figure 7. HRTEM micrographs of calcined HAp powders. (a) From the micelle porogen and (b) from the dendrimer porogen.

calcining at 600 °C to remove CTAB molecules. The mechanism would be the same even in the case of a PAMAM dendrimer porogen. A PAMAM−calcium phosphate cluster is formed after the addition of an aqueous PO_4^{3-} solution to the aqueous PAMAM solution and the addition of an aqueous Ca^{2+} solution to the aforementioned solution. Then mesoporous HAp powders are also obtained after the growth of HAp crystals by aging and calcining HAp powders at 600 °C (Scheme 1).

To functionalize the surfaces of HAp particles, the calcined HAp particles, which were synthesized using a micelle porogen, were modified by the PAMAM dendrimer. The FTIR absorption spectrum measurement was carried out to investigate the presence of dendrimer after the modification. Figure 8a shows an FTIR spectrum of PAMAM-dendrimer-

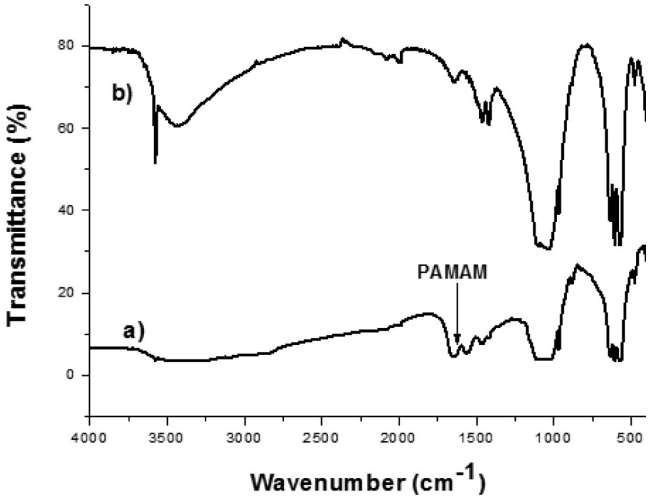

Figure 8. FTIR spectra of calcined HAp powders. (a) Surface modification with PAMAM dendrimer and (b) before surface modification.

modified HAp particles. The strong absorption bands at 1650 and 1550 cm^{-1}, which are assigned to amide I and II of the dendrimer, respectively,[52,54] are observed in this spectrum. However, these bands are absent in the spectrum for calcined HAp particles before modification (Figure 8b). Hence, it was confirmed by FTIR absorption spectra that HAp particles were modified with dendrimer.

To investigate the effect of pH on the coating, the surface modification of HAp particles by dendrimer was performed at different pH values. TEM micrographs (Figure 9a−d) certified

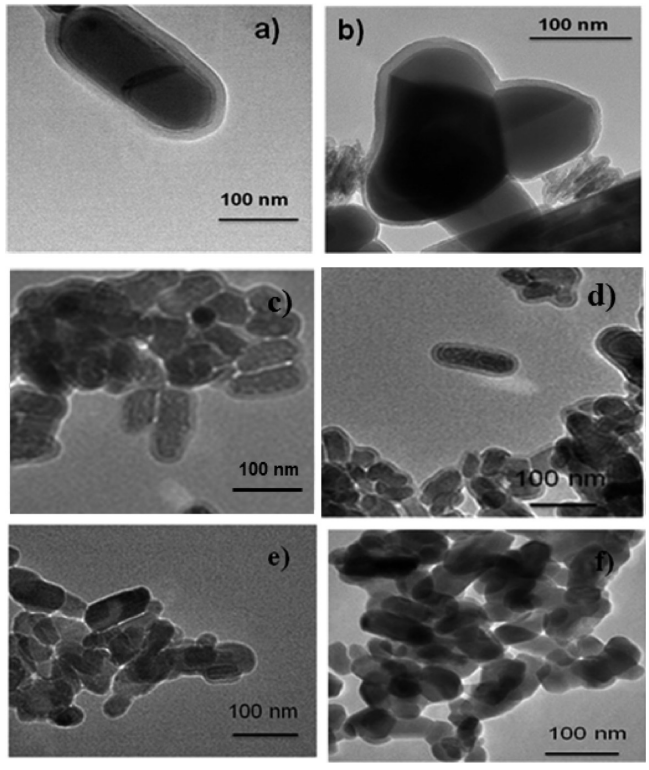

Figure 9. TEM micrographs of calcined HAp powders surface modified with PAMAM dendrimer. (a) pH 10.6, (b) pH 9.6, (c) pH 9.2, (d) pH 8.6, (e) pH 6.8, and (f) pH 3.8.

the shell layer on dendrimer-coated HAp particles. The result from the TEM study supports the result obtained from the FTIR study, which confirms the modification of particles with dendrimer. The thickness of the coating was evaluated from TEM images. At pH 10.6 and 9.6, the thickness of the coating was around 9 to 10 nm (Figure 9a,b). The shell thickness decreases with decreasing pH. It was approximately 6 to 7 nm at pH 8.6 (Figure 9d), but it decreased to around 3 to 4 nm at pH 7.5. The obtained thicknesses are plotted as a function of pH in Figure 10. The diameter of the PAMAM dendrimer (generation 4) is ∼4.5 nm.[32] Therefore, it can be noted that at

dx.doi.org/10.1021/la302066e | *Langmuir* 2012, 28, 14018−14027

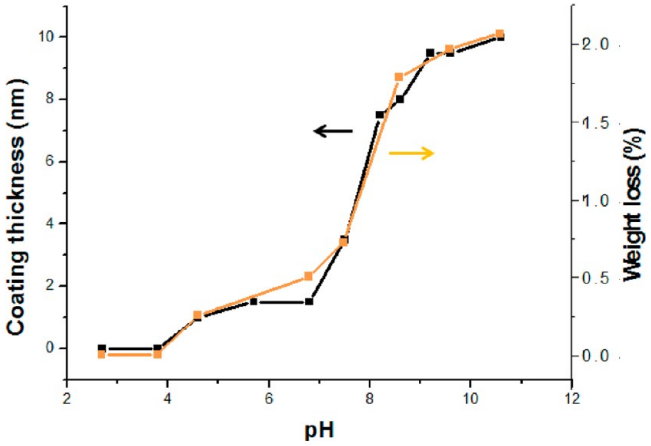

Figure 10. Coating thickness of dendrimer on the HAp surface and weight loss of HAp (at 600 °C) vs pH.

pH 9 or more about two layers of dendrimers coat the surfaces of HAp particles, but the thickness is only approximately one layer on the HAp surface at around pH 8. The average thickness was around 1 to 2 nm at pH 6.8 (Figure 9e). Moreover, under acidic conditions, the coating thickness became very thin and no thickness was observed below pH 4 (Figure 9f). The results clearly indicate that the coating is highly dependent on the pH. It should be noticed that the variation in thickness occurs between pH 9 and 6. Because the p*K*'s of primary and tertiary amines of dendrimer are 9.2 and 6.4,[55] the adsorption of dendrimer on HAp particles depends on the protonation of dendrimer, that is, nonprotonated or less-protonated dendrimers can easily adsorb or accumulate on the HAp surfaces.

To investigate the weight percent of coating, a TGA study was performed for the specimens obtained at different pH values. The decomposition of dendrimer occurred within the temperature range below 550 °C,[20] as revealed from the TGA curves (Figure 11). It was observed that the weight loss was larger for the specimens prepared at higher pH and decreased with decreasing pH. This indicates that the content of dendrimer decreases with decreasing pH. At lower pH (i.e., under acidic conditions), the weight loss is much less, indicating that a smaller amount of dendrimer coats the particle surface. The weight loss (at 600 °C) is plotted in Figure 10 for comparison with the coating thickness obtained from the TEM measurement after coating with the PAMAM dendrimer. The pH dependence of the weight loss is completely consistent with that of the coating thickness, and this result fully supports the pH-dependent surface modification by PAMAM dendrimer on HAp particles.

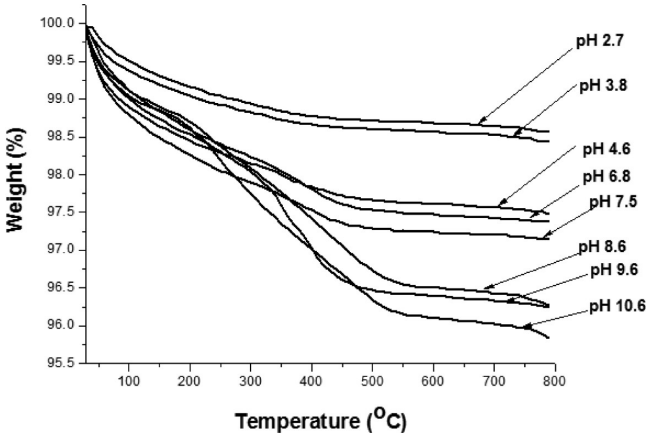

Figure 11. TG curves of calcined HAp powders surface modified with PAMAM dendrimer at different pH values.

It should be noticed that the pH dependency of the coating thickness and weight loss in Figure 10 is similar to the pH titration curve of the amine-terminated PAMAM dendrimer.[55] Then, the pH-dependent adsorption behavior of dendrimers on HAp can be assumed on the basis of protonation/deprotonation of the dendrimers. Because dendrimers are fully protonated under acidic conditions, they do not preferably adsorb on HAp. Because tertiary amines of dendrimers deprotonate at pH values above their pK_a (6.4), the hydrophobicity of dendrimers increases, and the adsorption of dendrimers on HAp begins above pH 7. At pH higher than the pK_a (9.2) of primary amine, the adsorption reaches its highest value. A small degree of adsorption will consist of monolayer formation by the chemisorption of dendrimer on HAp, and successive accumulation can occur by the physisorption of dendrimer that may come from hydrogen bonding between dendrimers. The intermolecular hydrogen bonding among amine and amide groups of dendrimers was assumed from the self-aggregation of dendrimers.[56]

The adsorption experiment of PAMAM and poly(propylene imine) dendrimes is performed on many different surfaces. The interaction of PAMAM dendrimers with supported lipid bilayers has been investigated to obtain kinetic and mechanistic data.[57] The adsorption of dendrimers has been examined even on glass, mica, gold, and silica.[58−62] The adsorption of poly(propylene imine) on glass increases with decreasing ionic strength and pH.[58] The adsorption of carboxyl-terminated PAMAM dendrimer on gold reaches its maximum (more than 25 nm) at pH 6.[61] Meanwhile, the maximum adsorbed amount of PAMAM dendrimers on silicon oxide surfaces increases with increasing pH.[62] This pH dependency is interpreted as an effect of the substrate and is quantitatively explained by the extended three-body random sequential adsorption model, which stipulates the importance of a three-body interaction acting between two adsorbing dendrimers and the charged substrate. Because the pH tendency of the present work resembles the last case rather than the former two, it may be possible to determine additional aspects of the adsorption mechanism of the PAMAM dendrimer on HAp with the random sequential adsorption model.

4. SUMMARY AND CONCLUSIONS

Mesoporous HAp's were successfully synthesized using the CTAB micelle and PAMAM dendrimer as a porogen through a hydrothermal precipitation technique. The physicochemical properties of HAp powders synthesized from different porogens have also been studied by means of various measurements. An XRD study confirms that the synthesized materials have a single-phase HAp crystal structure with approximate aspect ratios of 2.25 to 2.29, which are very supportive of aspect ratios from TEM. An EDX study mentions that the powders are stoichiometric with Ca^{2+}/PO_4^{3-} number ratios of 1.662 and 1.669 for dendrimer and micelle porogens, respectively. Low-angle XRD and BET studies indicate that the HAp products are mesostructured in nature. The specific surface area and pore volume are found to be 56−63 m^2/g and 0.18−0.19 cm^3/g, respectively, for calcined HAp's synthesized

dx.doi.org/10.1021/la302066e | *Langmuir* 2012, 28, 14018−14027

under different porogens. The calculation from the desorption branch of the isotherms based on a BJH model has a broad pore size distribution with average sizes ranging from 4.7 to 5.5 nm for both cases. These results imply that the pores are generated through the embedding of porogens. However, the careful insight differentiates the larger specific surface area and pore size of HAp powders of the dendrimer porogen from those of the micelle porogen.

The surface of mesoporous HAp particles was functionalized successfully with the PAMAM dendrimer. The modification is confirmed by FTIR absorption spectra and TGA. TEM analysis also displays the presence of dendrimer on the particle surfaces, and the coating is very dependent on the pH, which is also apparent from the TGA result. At higher pH, the coating thickness of dendrimer on the particle surface is higher, 9 to 10 nm, indicating the double-layer coating of dendrimer on the particle surfaces. The coating thickness decreases rapidly from pH 9 to 6, in agreement with the weight loss on TGA. These behaviors deeply involve the pH dependence on the protonation of amine groups in the dendrimer, the interaction between adsorbed dendrimers, and the nature of the interaction of the dendrimer with HAp.

On the basis of the results obtained, it can be remarked that these results may provide the basis for utilizing the synthesized mesostructured HAp materials in biomedical applications because of the biocompatibility of HAp. In particular, the developed dendrimer-encapsulated or dendrimer-functionalized mesoporous hydroxyapatite materials may possess potential upon application to biocomposite drug delivery systems and/or bone tissue engineering.

AUTHOR INFORMATION

Corresponding Author

*E-mail: imae@mail.ntust.edu.tw.

Notes

The authors declare no competing financial interest.

ACKNOWLEDGMENTS

This work was financially supported by the National Taiwan University of Science and Technology, Taiwan, under grant 100H451201. N.P. gratefully acknowledges the National Taiwan University of Science and Technology, Taiwan, for the financial support of a postdoctoral fellowship. We thank Prof. Jordi Esquena, IQAC/CSIC, Spain, for nitrogen adsorption experiments and his beneficial discussion.

REFERENCES

(1) Antonelli, D. M.; Ying, J. Y. Synthesis of a Stable Hexagonally Packed Mesoporous Niobium Oxide Molecular Sieve Through a Novel Ligand-Assisted Templating Mechanism. *Angew. Chem., Int. Ed.* **1996**, *35*, 426−430.

(2) Dong, A.; Ren, N.; Tang, Y.; Wang, Y.; Zhang, Y.; Hua, W.; Gao, Z. General Synthesis of Mesoporous Spheres of Metal Oxides and Phosphates. *J. Am. Chem. Soc.* **2003**, *125*, 4976−4977.

(3) Kresge, C. T.; Leonowicz, M. E.; Roth, W. J.; Vartuli, J. C.; Beck, J. S. Ordered Mesoporous Molecular Sieves Synthesized by a Liquid-Crystal Template Mechanism. *Nature* **1992**, *359*, 710−712.

(4) Guo, Y. P.; Zhou, Y.; Jia, D. C. Fabrication of Hydroxycarbonate Apatite Coatings with Hierarchically Porous Structures. *Acta Biomater.* **2008**, *4*, 334−342.

(5) Shi, X. T.; Wang, Y. J.; Ren, L.; Zhao, N. R.; Gong, Y. H.; Wang, D. A. Novel Mesoporous Silica-Based Antibiotic Releasing Scaffold for Bone Repair. *Acta Biomater.* **2009**, *5*, 1697−1707.

(6) Vecchio, K. S.; Zhang, X.; Massie, J. B.; Wang, M.; Kim, C. W. Conversion of Bulk Seashells to Biocompatible Hydroxyapatite for Bone Implants. *Acta Biomater.* **2007**, *3*, 910−918.

(7) Almirall, A.; Larrecq, G.; Delgado, J. A. A. Fabrication of Low Temperature Macroporous Hydroxyapatite Scaffolds by Foaming and Hydrolysis of an Alpha-TCP Paste. *Biomaterials* **2004**, *17*, 3671−3680.

(8) Brendel, T.; Engel, A.; Russel, C. Hydroxyapatite Coatings by a Polymeric Route. *J. Mater. Sci.: Mater. Med.* **1992**, *3*, 175−179.

(9) Chang, B.-S.; Lee, C.-K.; Hong, K.-S.; Youn, H.-J.; Ryu, H.-S.; Chung, S.-S.; Park, K.-W. Osteoconduction at Porous Hydroxyapatite with Various Pore Configurations. *Biomaterials* **2000**, *21*, 1291−1298.

(10) Walsh, D.; Furuzono, T.; Tanaka, J. Preparation of Porous Composite Implant Materials by in Situ Polymerization of Porous Apatite Containing-Caprolactoneor Methyl Methacrylate. *Biomaterials.* **2001**, *22*, 1205−1212.

(11) Kundu, B.; Sinha, M. K.; Mitra, M. K.; Basu, D. Fabrication and Characterization of Porous Hydroxyapatite Ocularimplant Followed by an in Vivo Study in Dogs. *Bull. Mater. Sci.* **2004**, *27*, 133−140.

(12) Tripathi, G.; Basu, B. A Porous Hydroxyapatite Scaffold for Bone Tissue Engineering: Physico-Mechanical and Biological Evaluations. *Ceram. Int.* **2012**, *38*, 341−349.

(13) Wang, H.; Zhai, L.; Li, Y.; Shi, T. Preparation of Irregular Mesoporous Hydroxyapatite. *Mater. Res. Bull.* **2008**, *43*, 1607−1614.

(14) Xia, Z.; Liao, L.; Zhao, S. Synthesis of Mesoporous Hydroxyapatite Using a Modified Hard-Templating Route. *Mater. Res. Bull.* **2009**, *44*, 1626−1629.

(15) He, W.; Li, Z.; Wang, Y.; Chen, X.; Zhang, X.; Zhao, H.; Yan, S.; Zhou, W. Synthesis of Mesoporous Structured Hydroxyapatite Particles Using Yeast Cells as the Template. *J. Mater. Sci.: Mater. Med.* **2010**, *21*, 155−159.

(16) Guo, Y.-P.; Guo, L.-H.; Yao, Y.-B.; Ning, C.-Q.; Guob, Y.-J. Magnetic Mesoporous Carbonated Hydroxyapatite Microspheres with Hierarchical Nanostructure for Drug Delivery Systems. *Chem. Commun.* **2011**, *47*, 12215−12217.

(17) Ng, S.; Guo, J.; Ma, J.; Loo, S. C. Synthesis of High Surface Area Mesostructured Calcium Phosphate Particles. *Acta Biomater.* **2010**, *6*, 3772−3781.

(18) Poh, C. K.; Ng, S.; Lim, T. Y.; Tan, H. C.; Loo, J.; Wang, W. In Vitro Characterizations of Mesoporous Hydroxyapatite as a Controlled Release Delivery Device for VEGF in Orthopedic Applications. *J. Biomed. Mater. Res. A* **2012**, 24 DOI: , 10.1002/jbm.a.34252.

(19) Renzo, F. D.; Cambon, H.; Dutartre, R. A. 28-Year-Old Synthesis of Micelle-Templated Mesoporous Silica. *Microporous Mater.* **1997**, *10*, 283−286.

(20) Tanglumlert, W.; Wongkasemjit, S.; Imae, T. Fabrication of Dendrimer Porogen-Capsulated Mesoporous Silica via Sol−Gel Process of Silatrane Precursor. *J. Nanosci. Nanotechnol.* **2009**, *9*, 1844−1850.

(21) Preinerstorfer, B.; Lubda, D.; Lindner, W.; Lämmerhofer, M. Monolithic Silica-Based Capillary Column with Strong Chiral Cation-Exchange Type Surface Modification for Enantioselective Non-Aqueous Capillary Electrochromatography. *J. Chromatogr., A* **2006**, *1106*, 94−105.

(22) Moriguchi, T.; Yano, K.; Nakagawa, S.; Kaji, F. Elucidation of Adsorption Mechanism of Bone-Staining Agent Alizarin Red S on Hydroxyapatite by FT-IR Microspectroscopy. *J. Colloid Interface Sci.* **2003**, *260*, 19−25.

(23) Liu, Q.; de Wijn, J. R.; van Blitterswijk, C. A. A Study on the Grafting Reaction of Isocyanates with Hydroxyapatite Particles. *J. Biomed. Mater. Res.* **1998**, *40*, 358−364.

(24) D'Andrea, S. C.; Fadeev, A. Y. Covalent Surface Modification of Calcium Hydroxyapatite Using *n*-Alkyl- and *n*-Fluoroalkylphosphonic Acids. *Langmuir* **2003**, *19*, 7904−7910.

(25) Tanaka, H.; Yasukawa, A.; Kandori, K.; Ishikawa, T. Modification of Calcium Hydroxyapatite Using Alkyl Phosphates. *Langmuir* **1997**, *13*, 821−826.

(26) Tanaka, H.; Watanabe, T.; Chikazawa, M.; Kandori, K.; Ishikawa, T. Surface Structure and Properties of Calcium Hydrox-

yapatite Modified by Hexamethyldisilazane. *J. Colloid Interface Sci.* **1998**, *206*, 205−211.
(27) Tanaka, H.; Watanabe, T.; Chikazawa, M.; Kandori, K.; Ishikawa, T. TPD, FTIR, and Molecular Adsorption Studies of Calcium Hydroxyapatite Surface Modified with Hexanoic and Decanoic Acids. *J. Colloid Interface Sci.* **1999**, *214*, 31−37.
(28) Borum, L.; Wilson, O. C., Jr. Surface Modification of Hydroxyapatite. Part II. Silica. *Biomaterials* **2003**, *24*, 3681−3688.
(29) Misra, D. N. Adsorption of Zirconyl Salts and Their Acids on Hydroxyapatite: Use of the Salts as Coupling Agents to Dental Polymer Composites. *J. Dent. Res.* **1985**, *12*, 1405−1408.
(30) Liu, Q.; de Wijn, J. R.; Bakker, D.; van Blitterswijk, C. A. Surface Modification of Hydroxyapatite to Introduce Interfacial Bonding with Polyactive™ 70/30 in a Biodegradable Composite. *J. Mater. Sci.: Mater. Med.* **1996**, *7*, 551−557.
(31) Wang, X.; Li, Y.; Wei, J.; de Groot, K. Development of Biomimetic Nano-Hydroxyapatite/Poly(hexamethylene adipamide) Composites. *Biomaterials* **2002**, *23*, 4787−4791.
(32) Tomalia, D. A.; Naylor, A. M.; Goddard, W. A. Starburst Dendrimers: Molecular-Level Control of Size, Shape, Surface Chemistry, Topology, and Flexibility from Atoms to Macroscopic matter. *Angew. Chem., Int. Ed. Engl.* **1990**, *29*, 138−175.
(33) Tsortos, A.; Nancollas, A. The Adsorption of Polyelectrolytes on Hydroxyapatite Crystals. *J. Colloid Interface Sci.* **1999**, *209*, 109−115.
(34) Mitra, A.; Imae, T. Nanogel Formation Consisting of DNA and Poly(amido amine) Dendrimer Studied by Static Light Scattering and Atomic Force Microscopy. *Biomacromolecules* **2004**, *5*, 69−73.
(35) Tsai, Y.-J.; Hu, C.-C.; Chu, C.-C.; Imae, T. Intrinsically Fluorescent PAMAM Dendrimer as Gene Carrier and Nanoprobe for Nucleic Acids Delivery: Bioimaging and Transfection Study. *Biomacromolecules* **2011**, *12*, 4283−4290.
(36) Ottaviani, M. F.; Bossmann, S.; Turro, N. J.; Tomalia, D. A. Characterization of Starburst Dendrimers by the EPR Technique. 1. Copper Complexes in Water Solution. *J. Am. Chem. Soc.* **1994**, *116*, 661−671.
(37) Balogh, L.; Tomalia, D. A. Poly(amidoamine) Dendrimer-Templated Nanocomposites. 1. Synthesis of Zerovalent Copper Nanoclusters. *J. Am. Chem. Soc.* **1998**, *120*, 7355−7356.
(38) Esumi, K.; Suzuki, A.; Yamahira, A.; Torigoe, K. Role of Poly(amidoamine) Dendrimers for Preparing Nanoparticles of Gold, Platinum, and Silver. *Langmuir* **2000**, *16*, 2604−2608.
(39) Manna, A.; Imae, T.; Aoi, K.; Okada, M.; Yogo, T. Synthesis of Dendrimer-Passivated Noble Metal Nanoparticles in a Polar Medium: Comparison of Size between Silver and Gold Particles. *Chem. Mater.* **2001**, *13*, 1674−1681.
(40) Naka, K.; Kobayashi, A.; Chujo, Y. Effect of Anionic 4.5-Generation Polyamidoamine Dendrimer on the Formation of Calcium Carbonate Polymorphs. *Bull. Chem. Soc. Jpn.* **2002**, *75*, 2541−2546.
(41) Lak, A.; Mazloumi, M.; Mohajerani, M.; Kajbafvala, A.; Zanganeh, S.; Arami, H.; Sadrnezhaad, S. K. Self-Assembly of Dandelion-like Hydroxyapatite Nanostructures via Hydrothermal Method. *J. Am. Ceram. Soc.* **2008**, *91*, 3292−3297.
(42) Bertinetti, L.; Tampieri, A.; Landi, E.; Ducati, C.; Midgley, P. A.; Coluccia, S.; Martra, G. Surface Structure, Hydration, and Cationic Sites of Nanohydroxyapatite: UHR-TEM, IR, and Microgravimetric Studies. *J. Phys. Chem. C* **2007**, *111*, 4027−4035.
(43) Yanbao, L.; Wiliana, T.; Tam, K. C. Synthesis and Characterization of Nanoporous Hydroxyapatite Using Cationic Surfactants As Templates. *Mater. Res. Bull.* **2008**, *43*, 2318−2326.
(44) Luo, X.; Imae, T. Synthesis of Mesoporous Iron Phosphate Using PAMAM Dendrimer as a Single Molecular Template. *Chem. Lett.* **2005**, *34*, 1132−1133.
(45) Rajkumar, M.; Sundaram, N. M.; Rajendran, V. In-Situ Preparation of Hydroxyapatite Nanorod Embedded Poly(vinyl alcohol) Composite and Its Characterization. *Int. J. Eng. Sci. Technol.* **2010**, *2*, 2437−2444.
(46) Zhou, Z. H.; Zhou, P. L.; Yang, S. P.; Yu, X. B.; Yang, L. Z. Controllable Synthesis of Hydroxyapatite Nanocrystals via a Dendrimer-Assisted Hydrothermal Process. *Mater. Res. Bull.* **2007**, *42*, 1611−1618.
(47) Tiemann, M.; Fröba, M. Mesoporous Aluminophosphates from a Single-Source Precursor. *Chem. Commun.* **2002**, 406−407.
(48) Brunauer, S.; Emmett, P.; Teller, E. Adsorption of Gases in Multimolecular Layers. *J. Am. Chem. Soc.* **1938**, *60*, 309−319.
(49) Yao, J.; Tjandra, W.; Chen, Y. Z.; Tam, K. C.; Mab, J.; Soh, B. Hydroxyapatite Nanostructure Material Derived Using Cationic Surfactant as a Template. *J. Mater. Chem.* **2003**, *13*, 3053−3057.
(50) Hammari, L. E.; Merroun, H.; Coradin, T.; Cassaignon, S.; Laghzizil, A.; Saoiabi, A. Mesoporous Hydroxyapatites Prepared in Ethanol-Water Media: Structure and Surface Properties. *Mater. Chem. Phys.* **2007**, *104*, 448−453.
(51) Imae, T.; Kamiya, R.; Ikeda, S. Formation of Spherical and Rod-like Micelles of Cetyltrimethylammonium Bromide in Aqueous NaBr Solutions. *J. Colloid Interface Sci.* **1985**, *108*, 215−225.
(52) Mitra, A.; Bhaumik, A.; Imae, T. Synthesis and Characterization of Nanoporous Silica Using Dendrimer Molecules. *J. Nanosci. Nanotechol.* **2004**, *14*, 1052−1055.
(53) Onuma, K.; Ito, A. Cluster Growth Model for Hydroxyapatite. *Chem. Mater.* **1998**, *10*, 3346−3351.
(54) Ito, M.; Imae, T.; Aoi, K.; Tsutsumiuchi, K.; Noda, H.; Okada, M. In Situ Investigation of Adlayer Formation and Adsorption Kinetics of Amphiphilic Surface-Block Dendrimers on Solid Substrates. *Langmuir* **2002**, *18*, 9757−9764.
(55) Leisner, D.; Imae, T. Polyelectrolyte Behavior of an Interpolyelectrolyte Complex Formed in Aqueous Solution of a Charged Dendrimer and Sodium Poly(L-glutamate). *J. Phys. Chem. B* **2003**, *107*, 13158−13167.
(56) Luo, X.; Imae, T. Photochemical Synthesis of Crown-Shaped Platinum Nanoparticles Using Aggregates of G4-NH2 PAMAM Dendrimer As Templates. *J. Mater. Chem.* **2007**, *17*, 567−571.
(57) Parimi, S.; Barnes, T. J.; Prestidge, C. A. PAMAM Dendrimer Interactions with Supported Lipid Bilayers: A Kinetic and Mechanistic Investigation. *Langmuir* **2008**, *24*, 13532−13539.
(58) van Duijvenbode, R. C.; Koper, G. J. M.; Böhmer, M. R. Adsorption of Poly(propylene imine) Dendrimers on Glass. An Interplay between Surface and Particle Properties. *Langmuir* **2000**, *16*, 7713−7719.
(59) Mecke, A.; Lee, I.; Baker, J. R., Jr.; Holl, M. M. B.; Orr, B. G. Deformability of Poly(amidoamine) Dendrimers. *Eur. Phys. J. E* **2004**, *14*, 7−16.
(60) Esumi, K.; Ichikawa, M.; Yoshimura, T. Adsorption Characteristics of Poly(amidoamine) and Poly(propylene imine) Dendrimers on Gold. *Colloids Surf., A* **2004**, *232*, 249−252.
(61) Ito, M.; Imae, T. Self-Assembled Monolayer of Carboxyl-Terminated Poly(amidaomine) Dendrimer. *J. Nanosci. Nanotechnol.* **2006**, *6*, 1667−1672.
(62) Cahill, B. P.; Papastavrou, G.; Koper, G. J. M.; Borkovec, M. Adsorption of Poly(amido amine) (PAMAM) Dendrimers on Silica: Importance of Electrostatic Three-Body Attraction. *Langmuir* **2008**, *24*, 465−473.